INTL JOURNAL OF ELECTRONICS AND TELECOMMUNICATIONS, 2024, VOL. 70, NO. 4, PP. 909-914
Manuscript received July 13, 2024; revised October 2024. doi: 10.24425/ijet.2024.152077

Optimizing the Signal-to-Noise Ratio using the Virtual Line of Sight and choosing the appropriate dimensions

Bushra Jarjees Qeryaqos, and Saad Ahmed Ayoob

***Abstract*—One potential candidate technology for Beyond 5G (B5G) networks is the reconfigurable intelligent surface (RIS), which is easy to install on existing infrastructure such as vehicles and buildings. Creating additional paths between the transmitter and receiver to improve the received signal accessible to the system is one of the significant uses of RIS. A virtual line of sight (VLOS) is established through the Tx-RIS-Rx link without the line of sight (LOS). RIS technology solves the problem of low coverage in millimeter-wave communications. This paper presents the effect of the signal-to-noise ratio by changing dimensions. In addition to finding the optimal values for the dimensions that give the optimal SNR, simulation results prove that the RIS height is greater than or equal to half the dimension between the sender and the receiver. It is recommended that the RIS height be greater than half the distance between the sender and the receiver.**

***Keywords*—reconfigurable intelligent surfaces; millimeter-wave environment; signal-to-noise ratio; RIS height; VLOS**

I. Introduction

THE goal of every generation of communicators is to use new technologies and strategies to accomplish the three main pillars. Decrease latency (response time) while increasing capacity and transmitting data. For example, scheduling algorithms were added in the fourth generation to organize better the work involved in reception and transmission [1][2]. CoMP technology was introduced to boost signal strength at the cell edge and use a higher modulation level for greater efficiency [3]-[5]. The fifth generation strives to accomplish these objectives using untapped spectrum bands [6]. The most prominent of these bands are millimeter waves [7]. Millimeter wave technology has had great success in increasing bandwidth and increasing data rates [8], but it suffers from significant losses due to increased frequency [9]. One of the main ways to meet high-speed traffic requirements is to use reconfigurable intelligent surfaces (RISs) to create an environment beneficial for wireless propagation [10]. However, high-frequency radio transmission has poor propagation conditions, large path loss, and can be easily blocked [11]. This problem is addressed by RISs, which are seen as an achievable solution. RISs are considered a new group of planar structures capable of processing and reflecting electromagnetic waves that fall on them [12].

The next generation of wireless systems operates in difficult propagation settings, such as the millimeter frequency bands, which create new, higher-data-rate bands [13]. Since millimeter-wave approaches have an abundance of bandwidth, they can handle large data rates, which wireless communication systems typically aim to achieve [14][15]. RIS systems were created to regulate the wireless communications environment to mitigate the many challenges of millimeter wave [16], such as millimeter-limited propagation characteristics, high-rise buildings in densely populated cities creating shadows, and NLOS communication, making high-frequency transmission difficult. A VLOS is created through a Tx-RIS-Rx link [17]. Establishing extra paths between the transmitter (Tx) and receiver (Rx) to improve the system's attainable received signal is one of the important uses of RIS as seen in Figure 1 [18].

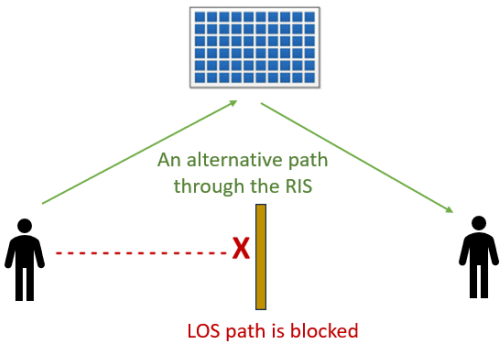

Fig. 1. VLOS via RIS

One potentially great feature of B5G telecom networks is RIS. It installs easily on vehicles and buildings and is reconfigurable as adaptive [19]. RIS arrays consist of several components that help beneficially modify the signal propagation environment and allow the formation of new pathways [20]. Since RIS can reflect or transmit digitally, it can be more adaptable to many communication expectations [21]. Since RIS does not require a transmitter unit but acts as a matrix to reflect the received signal, it does not require any time consumption [22]. RIS provides more bandwidth with low power consumption [23]. It can also prevent external influences not present in cellular environments by controlling intelligent variables over the network [24]. RIS helps to increase wireless communication coverage and throughput significantly [8]. As a result, RIS can improve the network, reduce power consumption, and solve the problem of poor coverage in millimeter transmission communications [25] [26].

The paper included several chief paragraphs after the introduction, including related work to the content of this

Authors are with University of Mosul, Iraq (e-mail: bushra.22enp75@student.uomosul.edu.iq, sa_ah_ay@uomosul.edu.iq).

manuscript. The third paragraph contained the communication model between the sender and receiver using a virtual line of sight. The results and discussion are in the fourth paragraph. Finally, the conclusions are in the fifth paragraph.

II. Related Work

Equations The importance of RIS becomes apparent when there is an obstacle between the sender and the recipient, as RIS provides alternative paths in the millimeter-wave environment. The dimensions between the transmitter (Tx) and the RIS and between the RIS and the receiver (Rx) vary to evaluate signal-to-noise ratio (SNR) values. These calculations are in cases where the transmitter beam footprint is smaller than the surface area [27]. Maximize the SNR, taking into account the RIS level transmission beam size and the RIS size in both scenarios: in the first, when the RIS is smaller than the fingerprint, and in the second case, when the RIS is larger than the fingerprint while accounting for beam losses. Moreover, an SNR comparison between the relay and the surface was performed. Through two scenarios, the optimal horizontal placement of the RIS to maximize the signal-to-noise ratio was found [28][29]. The proposed RIS system consists of 160 elements to operate in the anechoic region in the 5.8 GHz band and use a single flat-layer reflective array (FLRA) that can scan angles and elevation planes. FLRA integrates into a wireless communications system to examine beamforming gains, coverage improvements, and path loss in real-world outdoor communications environments [30]. Reference [31] illustrates how the size of the RIS can significantly affect the received power by presenting an analytical model that captures the RIS-assisted link performance. It also shows the relationship between the size of the RIS and the characteristics of the sender packet. Reference [32] addresses the problem of RIS deployment in 5G NR/6G cellular networks with directed antennas. Reference [33] examines downlink coverage with the aid of RIS. One base station (BS) and one user device (UE) make up this network. The proposed model for improving RIS placement maximizes cell coverage by optimizing the RIS direction by varying the horizontal distance between the RIS and the BS. In reference [34], the model introduced a new RIS design that allows for energy harvesting by using a subset of RIS unit cells (UCs) to divide the RIS unit cells to direct the beam. At the same time, the remaining UC units absorb energy. It seeks to improve the SNR of the receiver while adhering to RIS power consumption guidelines. In reference [35], a strategy has been proposed to reveal the optimal RIS position based on the relationship between the dimension from BS to UE and the dimension from the RIS to the BS-UE line to increase the strength of the received signal.

The comprehensive model variables are tested to obtain the effect of RIS height and to find the optimal RIS height that represents the goal of this work. One key variable includes different heights of the RIS to determine if it is located halfway between the sender and receiver to get the best SNR.

III. System Model

The proposed model can be described as containing a transmitter and a receiver, and between them, there is an obstacle to the transmitted signal. In other words, there is no line of sight between the sender and the receiver due to blocking or any obstacle in front of the signal, which prompts finding an alternative path for the signal through a path other than the line of sight. The reconfigurable intelligent surface (RIS) is proposed in this model to solve this problem in millimeter-wave communication systems. RIS is a passively reflective surface that requires no power source. The transmitter sends an electromagnetic wave to the receiver via the RIS. The RIS is in the form of a rectangle consisting of M×N elements, placed in the direction of the x and y axes, dx, dy. The spacing between the smart reflective surface elements is equal to λ /2.

Figure 2 shows the details of the studied system model in terms of significant dimensions and abbreviations. The coordinates of the transmitter, receiver, and RIS are (x_{TX}, y_{TX}, z_{TX}), (x_{RX}, y_{RX}, z_{RX}), and (x_{RIS}, y_{RIS}, z_{RIS}), respectively. The horizontal distance between the transmitter (Tx) and the receiver (Rx) is symbolized by (dh), and the horizontal distance between Tx and RIS is symbolized by dtsh or (d1). Directly, the symbol (dsrh) represents the horizontal distance between RIS and RX, the symbol (dts) represents the TX-RIS distance, and finally, the symbol represents the diagonal dimension RIS-RX with the symbol (dsr). The model relies heavily on the TX, RIS, and RX heights, which are denoted as ht, hs, and hr, respectively. The transmitted signal in VLOS is subjected to incidence and reflection angles θi and θr, respectively.

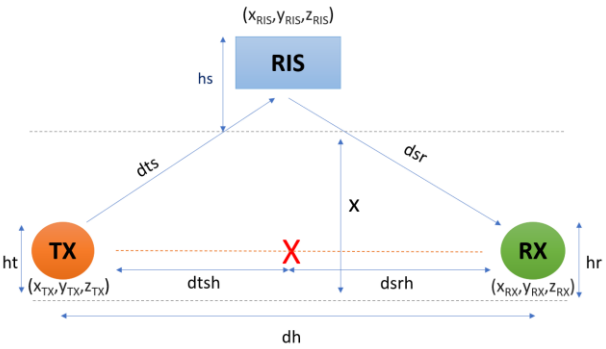

Fig. 2. A studied model.

As mentioned earlier, there is an obstacle between the sender and the receiver, and there is an NLOS path. The sender will send the signal to the RIS. The RIS will do its job of reflecting this signal to the receiver. These require that the position of the RIS be between the transmitter and the receiver, provided that the Tx and Rx are on the same side. Certainly, the sender and RIS must be in LOS on one side, and the RIS and receiver, on the other hand, must also be in LOS. The RIS must be higher than the transmitter and receiver heights to ensure that [28]. With the help of RIS, the SNR at the receiver is determined. Next, the optimal position of the RIS that gives the optimal SNR value will be determined through data analysis.

It is worth noting that the height of the transmitter and receiver are identical. In addition, path losses are taken into account. The surface is highly efficient and reflects the signal without any losses. The received power when placing the RIS between TX and RX calculates as follows [29]:

$$Pr = \frac{Pt\ Gt\ Gr\ \lambda^2\ \sigma}{(4\pi)^3 Dts^2 Dsr^2} \quad (1)$$

P_t is the transmitted power by the TX. Gt and Gr are the gains of the TX and RX antennas, respectively. The wavelength of the transmitted electromagnetic wave is λ. The dimensions between

TX-RIS and RIS-RX are dts and dsr. σ is the cross-section of the RIS that approximates a rectangular, planar surface. Detailed as follows:

$$\sigma = \frac{4\pi\eta Cos\theta i Cos\theta r A^2}{\lambda^2} \quad (2)$$

η is the efficiency of the RIS. A is the area of RIS. θi and θr represent the incident and reflected angles for the signal transmitted, respectively [36]. It is assumed in this paper that RIS consists of passive elements with η = 1. By substituting equation (2) into equation (1), the first equation takes on the following form:

$$Pr = \frac{Pt\ Gt\ Gr\ \eta\ A^2 Cos\theta i\ Cos\theta r}{(4\pi)^2 Dts^2 Dsr^2} \quad (3)$$

Consequently, it is possible to calculate the receiver's similar end-to-end SNR as:

$$SNR = \frac{Pr}{N_0} \quad (4)$$

Lastly, consider the presence of additive white Gaussian noise in the received signal, and symbolized by N_0 that the following equation uses to calculate it [27]:

$$N_o = -174 + 10\ log_{10}(w) + F_{dB} \quad (5)$$

Where W is the transmission bandwidth and F_{dB} is the noise figure in dB. Table I shows the parameters of the proposed model that were used in the simulation.

TABLE I
PARAMETERS OF THE PROPOSED MODEL

Labels	Parameter	Value
Operating frequency	f	28 GHz
Power Transmit	Pt	1 W
Signal bandwidth	W	2 GHz
Noise Figure	F_{dB}	10 dB
RIS efficiency	η	100%
Transmitter Gain	Gt	40 dB
Receiver Gain	Gr	10 dB
TX, RX height	ht, hr	2 m

IV. RESULTS AND DISCUSSION

This section contains results that support the analysis of the optimal placement of the RIS in a mm-wave environment. These results are obtained using equation (4) to validate the proposed system, as shown in Figure 2. It is worth noting that determining the optimal RIS position gives the maximum value of the acquired signal-to-noise ratio. In light of the analyzed calculations, it is easy to determine the following:

$$dts = \sqrt{dtsh^2 + x^2 + (hs - ht)^2} \quad (6)$$

$$dsr = \sqrt{dsrh^2 + x^2 + (hs - hr)^2} \quad (7)$$

$$\theta i = \tan^{-1}\left(\frac{\sqrt{dtsh^2 + (hs - ht)^2}}{x}\right) \quad (8)$$

$$\theta r = \tan^{-1}\left(\frac{\sqrt{dsrh^2 + (hs - hr)^2}}{x}\right) \quad (9)$$

Figure (3) shows the effect of high RIS on the SNR of the transmitted signal at different distances between the Tx and the Rx. If the RIS is placed midway between the transmitter and the receiver, for example, with x=5m as the reference [28], this shows how the SNR decreases as the RIS height increases.

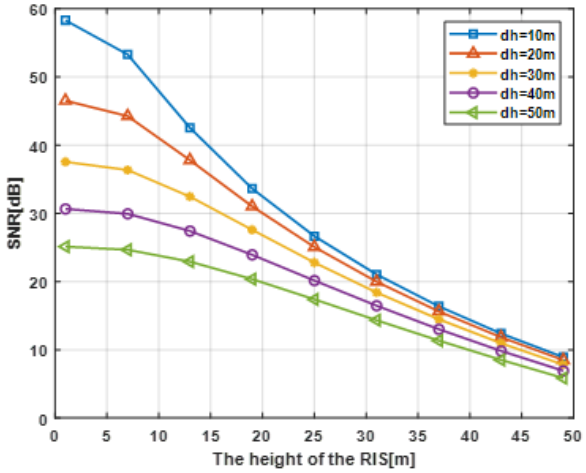

Fig.3. SNR varying with the height of RIS.

This paper uses the RIS at a specific height (hs) of 5 m, which represents the appropriate height, and a specific distance (x) of 5 m, which represents the horizontal distance between the Tx and the RIS. At these values, Figure 4(a) shows the effect of the distance between the sender and receiver on one side and the RIS on the other side. It is worth noting that the RIS is either close to the TX or the RX to obtain the maximum value of the SNR for several values of the distance (dh) between the TX and the RX of 20, 30, 40 and 50 m. The best result can be obtained when the RIS is in the middle (i.e., a distance (dh) of 10 m). It concluded that this height is small for distances (dh) exceeding 10 m. Therefore, the height (hs) of the RIS changed to 10 m. Unfortunately, the problem persists at distances of (x) 30, 40, and 50 m. Also, when using a distance (x) at 20 m, the SNR decreases at a horizontal TX-RX distance of 10 m.

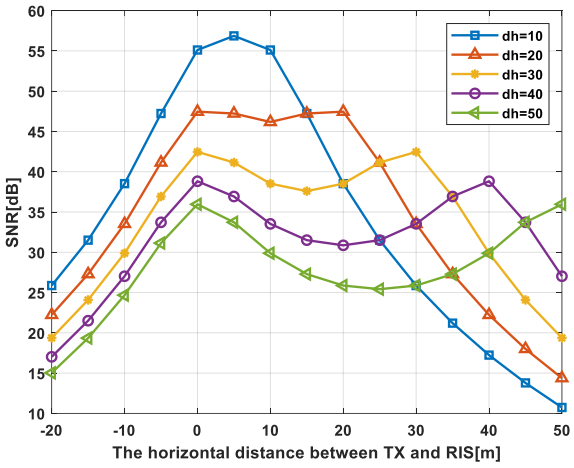

(a)

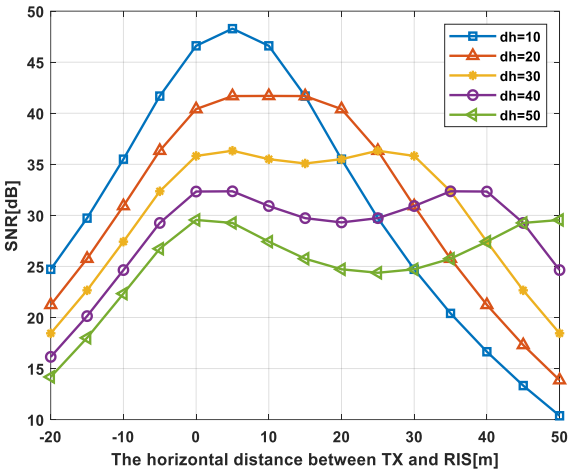

(b)

Fig.4. SNR varying with a horizontal distance (dtsh), (a) hs=5m, (b) hs=10m.

Figure 5 clearly shows the effect of height RIS on the SNR value. There are two cases. The first case is in which the height of the RIS is equal to a quarter of the distance between TX and RX. In this case, two peaks of SNR appear depending on the distance of the RIS to the Tx or the distance of the RIS to the Rx. If the RIS position is close to the sender, the peak appears near it. The same goes for the receiver. In other words, a concavity appears in the middle of the curve. The RIS height is half the distance between TX and RX in the second case, which is the critical case. Only one peak appears when the RIS position is in the middle. Therefore, the maximum SNR is obtained.

In the case where the height of the RIS is greater than the midpoint between the transmitter and the receiver, the maximum value of the SNR can be obtained when the RIS is midway between the Tx and the Rx, as shown in Figure 6. However, if the height is too high due to the increasing distance, the problem of a low SNR value will arise. The signal value decreases as the signal distance increases.

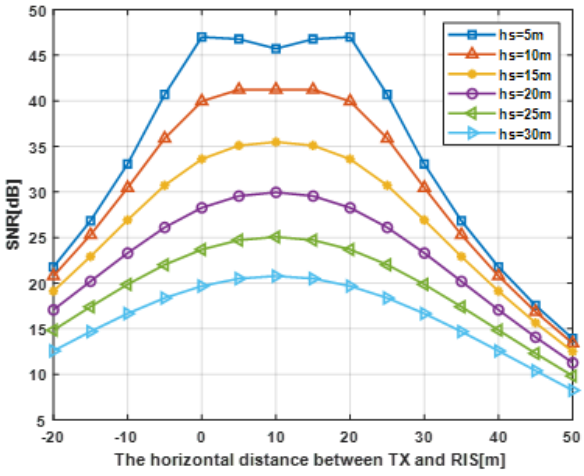

Fig. 5. SNR varying with a horizontal distance (dtsh) at the distance (dh=20m).

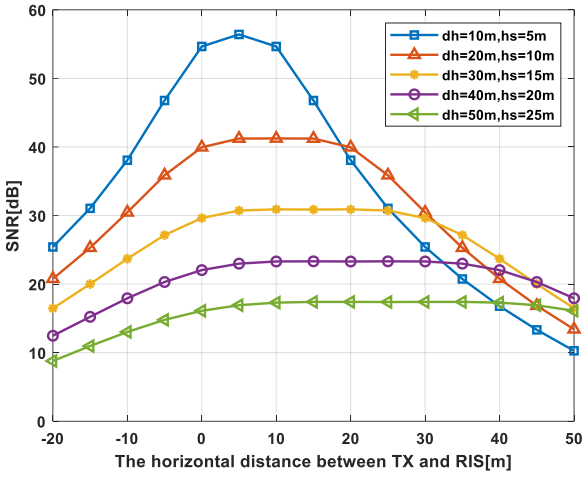

(a)

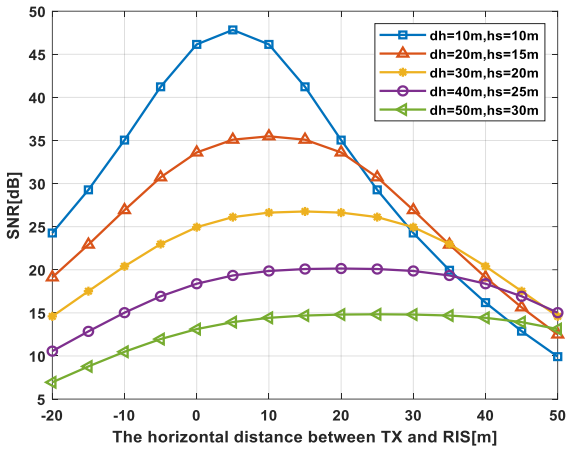

(b)

Fig.6. SNR varying with a horizontal distance between TX and RIS (dtsh), (a) hs = dh/2, (b) hs > dh/2

It is worth noting that the height of the surface must rise in proportion to the distance between the transmitter and the receiver. It leads to the conclusion that if the height of the RIS is equal to the middle of the distance between the TX and RX, then the best place for the RIS is in the middle of the distance between them or a place close to the middle. However, if the height of the RIS is greater than half the distance between them, the middle is the best place for the RIS.

CONCLUSION

The proposed model shows the effect of different dimensions on the SNR value. These various dimensions represent varying incident and reflection angles of the RIS. Furthermore, the goal when performing these experiments was to determine the appropriate height of the RIS to maximize the SNR. Clearly, the results showed that if the height of the RIS is equal to a quarter of the distance between the TX and the RX, the highest SNR value is obtained and occurs either when the RIS is close to the TX or the RX. If the height of RIS is equal to half the distance between TX and RX, this is the critical condition, which means that the maximum value of SNR can be obtained when RIS is in the middle. In the other case, if the RIS height is greater than the

midpoint between the transmitter and the receiver, the maximum value of SNR can be obtained when the RIS is midway between the transmitter and the receiver. In future work, we will study the effect of interference between transmitted beams. How can it be reduced?

ACKNOWLEDGEMENTS

Thanks to the University of Mosul for its continued support of postgraduate students.

REFERENCES

[1] J. Wu, D. Lin, G. Li, Y. Liu, Y. Yin, "Distributed Link Scheduling Algorithm Based on Successive Interference Cancellation in MIMO Wireless Networks," Wireless Communications and Mobile Computing, vol. 2019, 2019. https://doi.org/10.1155/2019/9083282

[2] M. A. Suliman, and S. A. Ayoob, "A comparison study between the downlink packet scheduling algorithms in LTE networks," Al-Rafidain Engineering Journal (AREJ), vol. 23, no. 3, pp. 27-40, 2015. https://doi.org/10.33899/rengj.2015.101568

[3] A.N Hammodat, and S.A. Ayoob, "Modelling and simulating of Coordinated Multi-Point (CoMP) technology in LTE-A. Journal of Computer Applications, 182(17), pp. 34-39, 2018. https://doi.org/10.5120/ijca2018917879

[4] S. Enoch, and I. Otung, "Performance Improvements in SNR of a Multipath Channel Using OFDM-MIMO," International Journal of Electronics and Telecommunications, vol. 69, no. 4, pp. 769-773, 2023. https://doi.org/10.24425/ijet.2023.147700

[5] F. S. Alsharbaty and S. A. Ayoob, "Intra-site CoMP Operation Effect of Fifth Generation Techniques on 802.16e Downlink Stream," International Journal of Engineering Trends and Technology, 67(4), pp. 12-17, 2019. https://doi.org/10.14445/22315381/IJETT-V67I4P204

[6] E. Basar, M. Di Renzo, J. De Rosny, M. Debbah, M. S. Alouini, and R. Zhang, "Wireless communications through reconfigurable intelligent surfaces," IEEE Access, vol. 7, no. June 2018, pp. 116753–116773, 2019. https://doi.org/10.1109/ACCESS.2019.2935192

[7] Z. Zhang et al., "Active RIS vs. Passive RIS: Which Will Prevail in 6G?," IEEE Trans. Communication, vol. 71, no. 3, pp. 1707–1725, 2023. https://doi.org/10.1109/TCOMM.2022.3231893

[8] Y. Wei, M. M. Zhao, M. J. Zhao, and Y. Cai, "Channel Estimation for IRS-Aided Multiuser Communications with Reduced Error Propagation," IEEE Trans. Wireless. Communication, vol. 21, no. 4, pp. 2725–2741, 2022. https://doi.org/10.1109/TWC.2021.3115161

[9] S. A. Ayoob, F. S. Alsharbaty, and A.N Hammodat, "Design and simulation of high efficiency rectangular microstrip patch antenna using artificial intelligence for 6G era," Telecommunication Computing Electronics and Control, vol. 21, no. 6, pp. 1234-1245, 2023. https://doi.org/10.12928/TELKOMNIKA.v21i6.25389

[10] A. A. A. Boulogeorgos and A. Alexiou, "Pathloss modeling of reconfigurable intelligent surface assisted THz wireless systems," IEEE Int. Conf. Communication., vol. 2, no. January, 2021. https://doi.org/10.1109/ICC42927.2021.9500473

[11] Y. Pan, C. Pan, S. Jin, and J. Wang, "RIS-Aided Near-Field Localization and Channel Estimation for the Terahertz System," IEEE J. Sel. Top. Signal Process., vol. 17, no. 4, pp. 878–892, 2023. https://doi.org/10.1109/JSTSP.2023.3285431

[12] M. A. Shawky et al., "Reconfigurable Intelligent Surface-Assisted Cross-Layer Authentication for Secure and Efficient Vehicular Communications," arXiv, pp. 1–12, 2023. https://doi.org/10.48550/arXiv.2303.08911

[13] S. A. Ayoob, F. S. Alsharbaty, and A. K. Alhafid, "Enhancement the heavy file application of 802.16 e cell using intra-site CoMP in uplink stream" Journal of Engineering Science and Technology, 17 (3), 1721-1733, 2022.

[14] C. Feng, W. Shen, J. An, and L. Hanzo, "Joint Hybrid and Passive RIS-Assisted Beamforming for mmWave MIMO Systems Relying on Dynamically Configured Subarrays," IEEE Internet Things J., vol. 9, no. 15, pp. 13913–13926, 2022. https://doi.org/10.1109/JIOT.2022.3142932

[15] R. A. Abed and S. A. Ayoob, "Millimeter Wave Beams Coordination and Antenna Array Height Effect," AIP Conference Proceedings, vol. 2830, no. 1, id.040003, pp. 11, 2023. https://doi.org/10.1063/5.0157290

[16] A. Al-Rimawi and A. Al-Dweik, "On the Performance of RIS-Assisted Communications with Direct Link Over κ-μ Shadowed Fading," IEEE Open J. Commun. Soc., vol. 3, no. November, pp. 2314–2328, 2022. https://doi.org/10.1109/OJCOMS.2022.3224562

[17] J. Rains et al., "High-Resolution Programmable Scattering for Wireless Coverage Enhancement: An Indoor Field Trial Campaign," IEEE Trans. Antennas Propag., vol. 71, no. 1, pp. 518–530, 2023. https://doi.org/10.1109/TAP.2022.3216555

[18] Y. Bian, D. Dong, J. Jiang, and K. Song, "Performance Analysis of Reconfigurable Intelligent Surface-Assisted Wireless Communication Systems Under Co-Channel Interference," IEEE Open J. Commun. Soc., vol. 4, no. February, pp. 596–605, 2023. https://doi.org/10.1109/OJCOMS.2023.3244648

[19] K. Singh, S. K. Singh, and C. P. Li, "On the Performance Analysis of RIS-Assisted Infinite and Finite Blocklength Communication in Presence of an Eavesdropper," IEEE Open J. Commun. Soc., vol. 4, no. February, pp. 854–872, 2023. https://doi.org/10.1109/OJCOMS.2023.3262485

[20] R. S. P. Sankar and S. P. Chepuri, "Optimal Placement of Active and Passive Elements in Hybrid RIS-assisted Communication Systems," pp. 1–5, 2023. https://doi.org/10.48550/arXiv.2301.06725

[21] Y. Wang, P. Guan, H. Yu, and Y. Zhao, "Transmit Power Optimization of Simultaneous Transmission and Reflection RIS Assisted Full-Duplex Communications," IEEE Access, vol. 10, pp. 61192–61200, 2022. https://doi.org/10.1109/ACCESS.2022.3179115

[22] Q. Wu and R. Zhang, "Intelligent Reflecting Surface Enhanced Wireless Network via Joint Active and Passive Beamforming," IEEE Trans. Wirel. Commun., vol. 18, no. 11, pp. 5394–5409, 2019, https://doi.org/10.1109/TWC.2019.2936025

[23] Q. Chen, M. Li, X. Yang, R. Alturki, M. D. Alshehri, and F. Khan, "Impact of residual hardware impairment on the iot secrecy performance of RIS-assisted NOMA networks," IEEE Access, vol. 9, pp. 42583–42592, 2021. https://doi.org/10.1109/ACCESS.2021.3065760

[24] N. Simmons et al., "A Simulation Framework for Cooperative Reconfigurable Intelligent Surface Based Systems," IEEE Transactions on Communications, vol. 72, no. 1, pp. 1–31, 2023. https://doi.org/10.1109/TCOMM.2023.3282952

[25] Y. Wang and J. Peng, "Energy Efficiency Fairness of Active Reconfigurable Intelligent Surfaces-Aided Cell-Free Network," IEEE Access, vol. 11, no. January, pp. 5884–5893, 2023. https://doi.org/10.1109/ACCESS.2023.3237213

[26] Z. Cui, K. Guan, J. Zhang, and Z. Zhong, "SNR Coverage Probability Analysis of RIS-Aided Communication Systems," IEEE Trans. Veh. Technol., vol. 70, no. 4, pp. 3914–3919, 2021. https://doi.org/10.1109/TVT.2021.3063408

[27] K. Ntontin, A. A. A. Boulogeorgos, D. G. Selimis, F. I. Lazarakis, A. Alexiou, and S. Chatzinotas, "Reconfigurable Intelligent Surface Optimal Placement in Millimeter-Wave Networks," IEEE Open J. Commun. Soc., vol. 2, pp. 704–718, 2021. https://doi.org/10.1109/OJCOMS.2021.3068790

[28] K. Ntontin, A. A. A. Boulogeorgos, D. G. Selimis, F. I. Lazarakis, A. Alexiou, and S. Chatzinotas, "Reconfigurable Intelligent Surface Optimal Placement in Millimeter-Wave Networks," IEEE Open J. Communications. Soc., vol. 2, no. March, pp. 704–718, 2021. https://doi.org/10.1109/OJCOMS.2021.3068790

[29] K. Ntontin, D. Selimis, A. A. A. Boulogeorgos, A. Alexandridis, A. Tsolis, V. Vlachodimitropoulos, and Fotis Lazarakis," Optimal Reconfigurable Intelligent Surface Placement in Millimeter-Wave Communications," 2021 15th European Conference on Antennas and Propagation (EuCAP), Dusseldorf, Germany, pp. 1-5, 2021. https://doi.org/10.23919/EuCAP51087.2021.9411076

[30] G. C. Trichopoulos et al., "Design and Evaluation of Reconfigurable Intelligent Surfaces in Real-World Environment," IEEE Open J. Commun. Soc., vol. 3, no. February, pp. 462–474, 2022. https://doi.org/10.1109/OJCOMS.2022.3158310

[31] G. Stratidakis, S. Droulias, and A. Alexiou, "Analytical Performance Assessment of Beamforming Efficiency in Reconfigurable Intelligent Surface-Aided Links," IEEE Access, vol. 9, pp. 115922–115931, 2021. https://doi.org/10.1109/ACCESS.2021.3105477

[32] G. Brancati, O. Chukhno, N. Chukhno, and G. Araniti, "Reconfigurable Intelligent Surface Placement in 5G NR/6G: Optimization and Performance Analysis," IEEE Int. Symp. Pers. Indoor Mob. Radio Communications PIMRC, vol. 2022-Septe, no. 6, 2022. https://doi.org/10.1109/PIMRC54779.2022.9978019

[33] S. Zeng, H. Zhang, B. Di, Z. Han, and L. Song, "Reconfigurable Intelligent Surface (RIS) Assisted Wireless Coverage Extension: RIS Orientation and Location Optimization," IEEE Communications. Letters., vol. 25, no. 1, pp. 269–273, 2021. https://doi.org/10.1109/LCOMM.2020.3025345

[34] K. Ntontin et al., "Wireless Energy Harvesting for Autonomous Reconfigurable Intelligent Surfaces," IEEE Transactions Green Communication. Netw., vol. 7, no. 1, pp. 114–129, 2023. https://doi.org/10.1109/TGCN.2022.3201190

[35] Y. Ren et al., "On Deployment Position of RIS in Wireless Communication Systems: Analysis and Experimental Results," IEEE Wireless Communications Letters, vol. 12, no. 10, pp. 1756–1760, 2023. https://doi.org/10.1109/LWC.2023.3292125

[36] I. Yildirim, A. Uyrus, and E. Basar, "Modeling and Analysis of Reconfigurable Intelligent Surfaces for Indoor and Outdoor Applications in Future Wireless Networks," IEEE Transactions on Communications, vol. 69, no. 2, pp. 1290–1301, 2021.
https://doi.org/10.1109/TCOMM.2020.3035391